Russian Research Centre "Kurchatov Institute"

V. G. Kohn

IAE-5878/9

THE THEORY OF X-RAY BRAGG-FRESNEL FOCUSING BY FLAT AND ELASTICALLY BENT LENS

e-mail: "kohn@kurm.polyn.kiae.su"
URL: "http://kohnvict.chat.ru"
Partially published in:
"A. Snigirev, V. Kohn, Proc. SPIE, vol.2516, p.29-37, 1995"

Moscow – 1995

УДК 548.732

Key words: X-rays, synchrotron radiation, Bragg-Fresnel optics, diffraction, focusing, elastically bent crystal.

A general theory of X-ray Bragg-Fresnel focusing by both the flat and the elastically bent perfect crystals having the phase zone relief on the surface in a sagittal direction is proposed for the explanation of the experimentally observed focusing effect. A general case of the X-ray spherical wave asymmetrical Bragg diffraction is considered. A small angle approximation is used for the description of the radiation transfer in the space between the Bragg-Fresnel lens and the observation plane. A special attention is paid to the consideration of the finite wavelength band of the radiation as well as the finite size of the source. It is shown that for a monochromatic incident wave the intensity on the topograph depends on the position along the focus line. This dependence is due to both the variation of the Bragg diffraction reflectivity and the change of the phase difference between the different phase zones. The existence of the wavelength band of the radiation leads to a homogeneous intensity distribution along the focus line. Each point of the line contains the contributions from all other points having the different intensity in the case of monochromatic wave. In the symmetrical case the lens of the finite length gives the image of the finite size. In an asymmetrical case the additional increase of the image size takes place. The meridional focusing by bent crystal gives the asymmetrical form of focus with the size of order of the micrometer.

1. Introduction

The optical devices play a very important role in various spheres of the human life and the science. The electromagnetic radiation of the different parts of the spectrum brings the unique information about the structure of the universe on one hand and about the inner structure of the nuclei on the the other hand. The appearance of the artificial powerful sources of the electromagnetic radiation at the synchrotron radiation beamlines opens the new branch of optics and stimulates the intensive investigation of new elements of the optical experimental arrangements.

For the parts of the electromagnetic radiation spectrum from a visual light up to soft X-rays the main coherent effects are the reflection and the refraction of the light beam at the boundary of two optically inhomogeneous media as well as the phase zone plates. As for the hard X-rays it is difficult to use these effects because of a very weak interaction of X-rays with a matter (the susceptibility lies within $10^{-6} - 10^{-5}$). As a consequence the very small reflection and refraction effects as well as the very small dimension of phase zones take place.

However for hard X-rays optics one has a new remarkable coherent effect, namely, the Bragg reflection by perfect single crystals. It opens the possibility to incline the X-ray beam by any angle with a hundred percent reflectivity within the narrow range of the angles of incidence of about few seconds of arc. This effect is used widely in different experimental arrangements for collimating and monochromazing the incident X-rays, especially, at the synchrotron radiation beamlines. The following development becomes possible thanks to a significant success in the technology of microstructuring which allows to create the arbitrary relief on the silicon single crystal surface with the teeth of about few micrometers height and from few to fraction of micrometer width. The combination of two effects, namely, the Bragg reflection and the phase zone focusing gives rise to the new optical device for hard X-rays – Bragg-Fresnel lens (BFL) which allows to obtain the line or point focus having the size of about tenth fraction of micrometer and to perform different transformation of angular properties of the incident synchrotron radiation beam.

The first proposal of Bragg-Fresnel optics was made in [1,2]. As a result of the experimental study it was foung that the best focusing effect arises in the geometry where the Bragg diffraction and phase zone focusing works in different directions [3-9]. In recent years the different applications of BFL on the ESRF (Grenoble) beamlines were performed (see the review [10] and references therein). Both the circular and linear BFL were used in the experiments. The circular BFL gives the point focus spot but it works in the arrangement of back scattering and therefore it is limited by the definite X-ray wavelength. The linear BFL gives the linear focus but it can be applied for various wavelengths. The change of wavelength leads only to the change of the Bragg angle and the focus distance. The combination of two perpendicularly oriented linear BFLs can give point focus as well.

Another way to obtain the point focus with a linear BFL is to use the elastically bent crystal. Such BFL combines the mirror focusing (in a meridional plane) and phase zone focusing (in a sagittal plane) and gives the focusing with a very high intensity inside the focus spot. First experimental testing the BFL of this type is performed in [11].

All the cited papers present the results of the experimental investigation of different properties of the Bragg-Fresnel lenses while the consequent theory is absent up to now. The goal of this article is just to present the general theory of hard X-ray Bragg-Fresnel optics. A general case of the spherical wave asymmetrical diffraction by elastically bent crystal having the phase surface relief in a sagittal plane is considered. A small angle approximation is used. A special attention is paid to the small deviations of the wavelength inside the narrow wavelength band of the previously monochromized incident radiation as well as to the positions of point sources within the limits of the source size.

2. General equations

The experimental arrangement is shown in Fig. 1. The spherical wave from the point $(\xi_s,\, \eta_s)$ at the source plane with a centre at the point S falls on the surface of a crystal plate of thickness t. The intensity of reflected wave is fixed by the film. The distance from the source to the crystal is L_0, the distance from the crystal to the film is L_1. Let us choose the reference coordinate system with the origin on the surface of the flat crystal so that the direction SO, which is represented by the unit vector $\boldsymbol{S}_0$, satisfies exactly the Bragg condition $(\boldsymbol{k}_0 + \boldsymbol{h})^2 = K^2$ where $\boldsymbol{k}_0 = K\,\boldsymbol{S}_0$, $K = 2\pi/\lambda_c$, λ_c is a centre of the considered wavelength band and $\boldsymbol{h}$ is the considered reciprocal lattice vector. The notation $\boldsymbol{k}_0 + \boldsymbol{h} = \boldsymbol{k}_1 = K\,\boldsymbol{S}_1$ will be used. The scattering plane is $(X,\, Z)$ and the vectors

$\boldsymbol{S}_0$, $\boldsymbol{S}_1$ have the coordinates $\boldsymbol{S}_0 = (\, c_0 \,, \, 0 \,, \, \gamma_0 \,)$, $\boldsymbol{S}_1 = (\, c_1 \,, \, 0 \,, \, -\gamma_1 \,)$. Here $c_0 = \cos\theta_0$, $c_1 = \cos\theta_1$, $\gamma_0 = \sin\theta_0$, $\gamma_1 = \sin\theta_1$, θ_0 is the angle between the direction $\boldsymbol{S}_0$ (incident beam) and the X-axis, θ_1 is the same for $\boldsymbol{S}_1$ (reflected beam).

The current wavelength value λ enters in the equations by means of wavenumber $2\pi/\lambda = K\,(1-\delta)$ where $\delta = (\lambda - \lambda_c)/\lambda = \Delta\lambda/\lambda$ is a small relative wavelength shift from the centre of the wavelength band. The high sensitivity of the diffraction effect makes it necessary to analyse the influence of the wavelength dispersion in an explicit form.

The intensity distribution on the topograph will be described in terms of the local coordinate system $(\xi,\, \eta)$ where η-axis coincides with Y-axis and η_s axis while ξ-axis is normal to the $\boldsymbol{S}_1$ direction. Similarly the ξ_s axis is normal to the $\boldsymbol{S}_0$ direction. To analyse the diffraction inside the crystal by means of Takagi equations [12] the oblique-angled coordinates s_0, s_1 will be considered which are determined by the relation $\boldsymbol{r} = s_0\boldsymbol{S}_0 + s_1\boldsymbol{S}_1$. It is easy to obtain that $x = c_0\, s_0 + c_1\, s_1$, $z = \gamma_0\, s_0 - \gamma_1\, s_1$.

The Bragg angle is $\theta_B = (\theta_0 + \theta_1)/2$. The notation $\gamma = \sin 2\theta_B$ will be used as well. For the sake of simplicity only the case of σ-polarised radiation will be considered. In the case of π-polarisation only an additional polarisation multiplier will arise. In our case the solution of Maxwell's equation inside the crystal volume can be written in the form

$$E(\boldsymbol{r}) = E_0(\boldsymbol{r})\, \exp\left(i\boldsymbol{k}_0\boldsymbol{r}\right) + E_1(\boldsymbol{r})\, \exp\left(i\boldsymbol{k}_1\boldsymbol{r}\right) \tag{1}$$

After substituting (1) in the Maxwell's equation and eliminating the rapid oscillations by taking into account the crystal periodicity and the small value of scattering amplitude by an individual atom one can obtain the well known Takagi equations [12] in the following form

$$\begin{aligned} \frac{dE_0}{ds_0} + iK\delta\, E_0 &= \frac{i}{2} K\, \left[\, \chi_0\, E_0 + \chi_{\bar{h}} \exp\left(i\boldsymbol{h}\boldsymbol{u}\right) E_1 \,\right], \\ \frac{dE_1}{ds_1} + iK\delta\, E_1 &= \frac{i}{2} K\, \left[\, \chi_h \exp\left(-i\boldsymbol{h}\boldsymbol{u}\right) E_0 + \chi_0\, E_1 \,\right], \end{aligned} \tag{2}$$

where χ_0, χ_h, $\chi_{\bar{h}}$ are zero, $\boldsymbol{h}$ and $-\boldsymbol{h}$ Fourier components of the crystal susceptibility. The derivatives over the oblique-angled coordinate mean the following

$$\frac{d}{ds_0} = c_0\, \frac{d}{dx} + \gamma_0\, \frac{d}{dz}\,, \qquad \frac{d}{ds_1} = c_1\, \frac{d}{dx} - \gamma_1\, \frac{d}{dz} \tag{3}$$

The phase factor $\exp\left(i\boldsymbol{h}\boldsymbol{u}\right)$ describes the additional phase due to atoms desplacement in the lattice of elastically bent crystal plate.

The boundary of the crystal is the plane at $z = 0$ which corresponds to the top of the surface relief (see Fig.1). The nondiffracting areas under the plane $z = 0$ will be taken into account as the areas with $\chi_0 = \chi_h = 0$ in solving the Takagi equations. Therefore it is sufficient to put the amplitude of the incident wave $A(x, y) = E_0(x, y, 0)$ as the boundary condition. The result of solution of the Takagi equations must be the function $B(x, y) = E_1(x, y, 0)$ at the same plane.

Let us determine the function $A(x, y)$ for the case of the spherical wave from the source at the point (ξ_s, η_s). If the source is placed at the distance L_0 from the sample then the vector $\boldsymbol{r}$ from a point at the source to the surface of the crystal has the expression $\boldsymbol{r} = L_0 \boldsymbol{S}_0 + x \boldsymbol{X} - \xi_s \boldsymbol{\xi}_s + (y - \eta_s) \boldsymbol{Y}$ where $\boldsymbol{X}$, $\boldsymbol{Y}$ and $\boldsymbol{\xi}_s$ are the unit vectors along the corresponding axes. Taking into accout the explicit form of $\boldsymbol{S}_0$ (see above) and $\boldsymbol{\xi}_s$ one has

$$r = \sqrt{\boldsymbol{r}^2} \approx L_0 + x\, c_0 + \frac{1}{2L_0} \left[\, (x\gamma_0 - \xi_s)^{\,2} + (y - \eta_s)^2 \,\right] \tag{4}$$

Because of $\boldsymbol{k}_0 \boldsymbol{r} = K\, x\, c_0$ at the surface of the crystal one obtains

$$\frac{\exp\left(2\pi i\, r/\lambda\right)}{r} \approx A(x, y)\, \exp\left(i\, \boldsymbol{k}_0 \boldsymbol{r}\right) \tag{5}$$

with $A(x, y) = A_1(x)\, A_2(y)$ where

$$\begin{aligned} A_1(x) &= \frac{F_0}{\sqrt{L_0}} \exp\left(-iK\delta c_0\, x + i\, \frac{K}{2L_0}\, (x\gamma_0 - \xi_s)^{\,2}\right), \\ A_2(y) &= \frac{1}{\sqrt{L_0}} \exp\left(i\, \frac{K}{2L_0}\, (y - \eta_s)^2\right). \end{aligned} \tag{6}$$

Here $F_0 = \exp\left(i\, K\, L_0\, (1 - \delta)\,\right)$ is an invisible phase multiplier.

The field passage through the air from the surface of the crystal to the film, where the focusing effect may be looking for, can be described by means of standard technique of plane waves expansion. In this way one represents the field at the surface of the crystal as the two-dimensional Fourier integral. Then z coordinate along the normal to the surface is introduced so that the vector $\boldsymbol{k}$ in the phase $\boldsymbol{k}\boldsymbol{r}$ has z-component which is determined from the condition that the modulus of $\boldsymbol{k}$ must be equal to $2\pi/\lambda$. Then passing to the coordinates ξ and η in the film plane and making the inverse Fourier transformation one can obtain

$$C(\xi, \eta) = \int dxdy\, G(\xi, \eta, x, y)\, B(x, y) \tag{7}$$

with

$$G(\xi,\eta,x,y) = \frac{K\gamma_1 F_1}{2\pi i L_1} \exp\left(iK\delta c_1\, x + \right.$$
$$\left. + i\frac{K}{2L_1}\left[\,(\xi - x\,\gamma_1)^{\,2} + (\eta - y)^{\,2}\,\right]\right), \tag{8}$$

where $F_1 = \exp\left(iKL_1\,(1-\delta)\right)$ is another invisible multiplier.

3. Bragg reflection by elastically bent crystal plate.

The elastically bent crystal plate of thickness t with the curvature radius R_c in the scattering plane $(X,\,Z)$ (see Fig.1) is decribed by the field of displacement $\boldsymbol{u}(x,z)$. It is well known (see, for example, [13]) that the general solution of the equation of the unisotropic elasticity theory gives the following expression for the vector $\boldsymbol{u}(x,z)$.

$$u_x = \frac{x}{R_c}\,(z-\frac{t}{2}) - \frac{A_{11}}{2R_c}\,(z-\frac{t}{2})^2\,,$$
$$u_z = -\,\frac{x^2}{2R_c} - \frac{A_{31}}{2R_c}\,(z-\frac{t}{2})^2\,, \tag{9}$$

where A_{11}, A_{31} are some combinations of the elastic compliance tensor components (see, for example, [14])

With taking into account the relation $\boldsymbol{h} = K(\boldsymbol{S}_1 - \boldsymbol{S}_0)$ we write the phase $\boldsymbol{hu}$ in the form $\boldsymbol{hu} = \Phi_0 + \Phi_1$, where

$$\Phi_0(x,z) = -\,\frac{Kc_0}{R_c}\,x\,z_t + \frac{K\gamma_0}{2R_c}\,x^2 + \frac{Ka_0}{2R_c}\,z_t^2 = -\boldsymbol{k}_0\boldsymbol{u}\,,$$
$$\Phi_1(x,z) = +\,\frac{Kc_1}{R_c}\,x\,z_t + \frac{K\gamma_1}{2R_c}\,x^2 + \frac{Ka_1}{2R_c}\,z_t^2 = \boldsymbol{k}_1\boldsymbol{u}\,, \tag{10}$$

where $z_t = z - t/2$, $a_0 = c_0A_{11} + \gamma_0A_{31}$, $a_1 = -c_1A_{11} + \gamma_1A_{31}$.

To obtain the solution of Takagi equations (2) with the displacement field (10) let us make the substitution

$$E_0 = E_0'\,\exp(i\Phi_0)\,,\quad E_1 = E_1'\,\exp(-i\Phi_1)\,. \tag{11}$$

It is easy to verify that the derivatives of the phases Φ_m $(m = 0,1)$ along the direction $\boldsymbol{S}_m$ does not depend on x. The Takagi equations for the new fields E_0' and E_1' take the form

$$\left[\frac{d}{ds_0} + iK\delta - i\,\frac{Ka_0'}{R_c}\,z_t\right]\,E_0' = \frac{i}{2}\,K\left[\,\chi_0\,E_0' + \chi_{\bar{h}}\,E_1'\,\right],$$
$$\left[\frac{d}{ds_1} + iK\delta - i\,\frac{Ka_1'}{R_c}\,z_t\right]\,E_1' = \frac{i}{2}\,K\left[\,\chi_h\,E_0' + \chi_0\,E_1'\,\right], \tag{12}$$

where $a_0' = c_0^2 - \gamma_0 a_0$, $a_1' = c_1^2 - \gamma_1 a_1$.

Correspondingly, the boundary condition for the field E_0' takes the form

$$A_1'(x) = \frac{F_0 F_0'}{\sqrt{L_0}} \exp\left(-iq_0 x + i\,\frac{x^2}{2\alpha_0}\right) . \qquad (13)$$

Here and below the following notations are used

$$\begin{aligned}
&q_0 = K\left(\delta_t c_0 + \frac{\gamma_0 \xi_s}{L_0}\right) , \quad \delta_t = \delta + \frac{t}{2R_c} , \\
&\alpha_m = \frac{L_m}{K\gamma_m^2 M_m} , \quad M_m = \left(1 - \frac{L_m}{\gamma_m R_c}\right) , \quad m = 0,\, 1 , \\
&F_0' = \exp\left(iK\left[\frac{\xi_s^2}{2L_0} - \frac{a_0 t^2}{8R_c}\right]\right) . \qquad (14)
\end{aligned}$$

The solution of the equations (12) can be found by means of standard technique of the variables x and z separation. For this purpose we represent the boundary condition (13) as the Fourier integral

$$A_1'(x) = \int \frac{dq}{2\pi}\, A_1'(q)\, \exp(iqx) \qquad (15)$$

with

$$\begin{aligned}
A_1'(q) &= \int dx\, A_1'(x)\, \exp(-iqx) \; = \\
&= \frac{F_0 F_0'}{\gamma_0} \left(\frac{2\pi i}{KM_0}\right)^{\frac{1}{2}} \exp\left(-i\,\frac{\alpha_0}{2}\,(q+q_0)^{\,2}\right) , \qquad (16)
\end{aligned}$$

Here and below a table integral is used (see, for example, [15, 16])

$$\int_{-\infty}^{\infty} dx\, \exp(iax + ibx^2) = \left(\frac{\pi i}{b}\right)^{\frac{1}{2}} \exp\left(-i\,\frac{a^2}{4b}\right) \qquad (17)$$

Then the solution of (12) can be represented in the form of the same Fourier integral (15) in which the integrand will contain the solution of (12) with the plane-wave boundary condition $A_1'(x) = \exp(iqx)$. This solution can be found in the form similar to the case of the flat crystal

$$\begin{aligned}
E_0'(x,z) &= E_0'(q,z)\, \exp\,(iqx)\,, \\
E_1'(x,z) &= E_0'(q,z)\, R(q,z)\, \exp\,(iqx) \qquad (18)
\end{aligned}$$

with $E_0'(q,0) = 1$. Substituting (18) in (12) and eliminating the function $E_0'(q,z)$ from the equations one can obtain the following nonlinear equation for R

$$\frac{dR}{dz} = i(\sigma_0 - \sigma_1 z)R - i\,\frac{s}{2}\,[1 + fR^2] \tag{19}$$

where

$$\begin{aligned}
&\sigma_0 = \frac{q\,\gamma}{\gamma_0\gamma_1} - X + v\,, \quad X = K\chi_0\,\frac{(\gamma_0+\gamma_1)}{2\gamma_0\gamma_1}\,,\\
&v = K\delta\,\frac{(\gamma_0+\gamma_1)}{\gamma_0\gamma_1} + \sigma_1\frac{t}{2}\,, \quad \sigma_1 = \frac{K}{R_c}\left(\frac{a_0'}{\gamma_0} + \frac{a_1'}{\gamma_1}\right)\,,\\
&s = \frac{K\chi_h}{\gamma_1}\,, \qquad f = \frac{\gamma_1\chi_{\bar h}}{\gamma_0\chi_h}\,.
\end{aligned} \tag{20}$$

It is well known that in the Bragg case of X-ray diffraction the reflected beam is formed inside the thin layer of thickness about an extinction length $L_{ex} = (s\sqrt{f}\,)^{-1}$ near the surface. At the depth L_{ex} depending on z term yields the phase $\psi = \sigma_1 L_{ex}^2/2$. It can be expressed in the case of the symmetrical diffraction $\gamma_0 = \gamma_1 = \sin\theta_B$ as $\psi = (2\pi L_{ex}^2)/(\lambda R_c \sin\theta_B)$. In this work only small bending of the crystal will be considered. Typical values of the parameters $L_{ex} = 1.5\,\mu m$, $\lambda = 1\,\text{Å}$, $R_c = 10\,\text{m}$ and $\sin\theta_B = 0.2$ lead to $\psi = 0.07$. Therefore in the case of large radius of curvature one can neglect the depending on z term in the equation and use the known solution for the perfect crystal. Then bending shows itself in the R-function only by means of shift of the Bragg angle depending on the thickness of the crystal plate. The exact numerical solution of the Eq.(19) for different values of bending radius obtained in [17] corresponds to this suggestion. It is interesting to notice that the Eq.(19) has the analytical solution through the Weber function which was found for the first time in [18, 19]. The exact analytical solution of Eq.(19) see in Appendix.

Thus the solution of Eq.(19) in the limit $\sigma_1 z = 0$ will be considered below which just corresponds to the flat crystal. This solution in the case of thick absorbing crystal plate has the form

$$R(q) = \frac{1}{sf}\,[\,\sigma_0 \pm \sqrt{\sigma_0^2 - fs^2}\,] \tag{21}$$

The solution takes place at the real surface of the crystal. If the surface has the phase relief in the form of a stripe parallel to the scattering plane (along the X-axis, see Fig.1) then at the places of etching the crystal the plane $z = 0$ of boundary condition and the real surface of the crystal will be divided by air layer of thichness d. In this case the additional solution of (19) is necessary inside the air layer where $\chi_0 = \chi_h = 0$ and the equation takes the simple form $dR/dz = i\sigma'_0 R$ where σ'_0 equals σ_0 without the term containing χ_0. Since the function (21) is dependless on z solution of (19), it is easy to understand that we have to solve the Takagi equation inside the air layer with the boundary condition (21). As a result the air layer brings the additional phase $-iqx_d - ivd$ to this solution where d depends on y and $x_d = d\gamma/\gamma_0\gamma_1$.

The formulae obtained allow to write the total solution of the Takagi equations (2) with the displacement field (9) in the next approximate form

$$B(x,y) = A_2(y)\,\exp\{-i\Phi_1(x,0) - ivd\}\,\frac{F_0F'_0}{\gamma_0}\left(\frac{2\pi i}{KM_0}\right)^{\frac{1}{2}} \times$$
$$\times \int \frac{dq}{2\pi}\,R(q)\,\exp\left(iq(x-x_d) - \frac{\alpha_0}{2}\,(q+q_0)^2\right)\,. \qquad (22)$$

In the following consideration the integral in (22) will be estimated approximately by means of the stationary phase method. The main contribution to the integral is brought by the region closed to the point $q = q_s(x,d)$ where the first derivative of the phase over q equals zero. This point is determined by $q_s(x,d) = (x - x_d)/\alpha_0 - q_0$. Regarding the function $R(q)$ as the slow one it can be replaced by $R(q_s)$ and the remained integrand can be calculated explicitly. As a result one obtains obviously the function $A'_1(x - x_d)$, i.e.

$$B(x,y) = A_2(y)\,A'_1(x-x_d)\,R(q_s(x,d))\,\exp(-i\Phi_1(x,0) - ivd)\,, \qquad (23)$$

where $A'_1(x)$ is determined by (13).

Substitution of (23) into (7) with taking into account (8), (13) leads to the following expression for the radiation field at the plane of observation

$$C(\xi,\eta) = \frac{F_0F_1F'_0F'_1\,K\gamma_1}{2\pi i\,L_1\sqrt{L_0}}\int dy\,\exp\left(i\,\frac{K}{2L_1}\,(\eta-y)^2 - ivd\right) \times$$
$$\times\, A_2(y)\int dx\,R(q_s(x,d))\,\exp(i\Psi(x,d)\,)\,, \qquad (24)$$

where

$$F'_1 = \exp\left(iK\left[\frac{\xi^2}{2L_1} - \frac{a_1t^2}{8R_c}\right]\right)\,,$$

$$\Psi(x,d) = -q_0(x-x_d) + q_1 x + \frac{(x-x_d)^2}{2\alpha_0} + \frac{x^2}{2\alpha_1}\,,$$
$$q_1 = K\left(\delta_t c_1 - \frac{\gamma_1 \xi}{L_1}\right)\,. \qquad (25)$$

Let us consider first the case where the focusing condition is not met. Then the integral over x in (24) can be estimated approximately by means of the stationary phase method once again. The point which brings the main contribution to the integral is determined from the condition $d\Psi/dx = 0$ and it equals

$$x = \frac{L_1}{L_x} M_0 x_d + \frac{L_0 L_1}{K L_x \gamma_0^2}\,(q_0 - q_1)\,, \qquad (26)$$

where

$$L_x = L_1 M_0 + L_0 M_1 \frac{\gamma_1^2}{\gamma_0^2} = L_1 + L_0 \frac{\gamma_1^2}{\gamma_0^2} - \frac{L_0 L_1 (\gamma_0 + \gamma_1)}{R_c\,\gamma_0^2}\,. \qquad (27)$$

Taking out the function $R(q_s(x,d))$ at the point (26) from the integral and calculating the rest integrand one can obtain with taking (6) into account

$$C(\xi,\eta) = \frac{\gamma_1}{\gamma_0}\,\frac{F_{inv}(\xi)}{(i\lambda L_x L_0 L_1)^{\frac{1}{2}}} \int dy\, R(q_s(\xi,d)) \times$$
$$\times \exp\{i\varphi_{tra}(y) - i\varphi_{fre}(\xi,d)\}\,, \qquad (28)$$

where F_{inv} is the invisible multiplier which vanishes in the intensity (nevertheless, it can be essential in considering the following passage of the coherent wave), φ_{tra} is the phase describing the transfer in y direction, φ_{fre} is the additional phase which is brought by the Fresnel surface relief. These and other parameters are determined by the following expressions

$$F_{inv}(\xi) = F_0 F_1 F_0' F_1' \exp\left(-i\,\frac{L_0 L_1 (q_0 - q_1)^2}{2K\gamma_0^2 L_x}\right)\,,$$
$$\varphi_{tra}(y) = \frac{K}{2}\left[\frac{(y-\eta_s)^2}{L_0} + \frac{(\eta - y)^2}{L_1}\right]\,,$$
$$\varphi_{fre}(\xi,d) = wd\,(\xi - \xi_{m\lambda} - \xi_s') - \varepsilon(d)\,,$$
$$q_s(\xi,d) = \frac{K M_0 \gamma_1}{L_x}\,(\xi - \xi_\lambda - \xi_d - \xi_s')\,,$$
$$w = \frac{K M_0 \gamma}{L_x \gamma_0}\,, \quad \varepsilon(d) = \frac{\gamma^2\, d^2}{\gamma_0^2\,\lambda\, L_x}\, M_0 M_1\,,$$

$$\xi_{m\lambda} = \xi_\lambda - \frac{v}{w}\,, \quad \xi_\lambda = \delta_t \left(L_1 \frac{c_1}{\gamma_1} + L_0 \frac{M_1\gamma_1 c_0}{M_0\gamma_0^2} \right)\,,$$

$$\xi_d = x_d\gamma_1 M_1 = dM_1 \frac{\gamma}{\gamma_0}\,, \quad \xi_s' = \xi_s \frac{\gamma_1 M_1}{\gamma_0 M_0}\,, \tag{29}$$

The result obtained is valid for the flat crystal as well in the limit $R_c = \infty$. The Eq.(28) is similar to that obtained in the small angle approximation in the theory of phase zone plate. Significant differencies arise in both the X-ray beam reflectivity and the formation of the additional phase which depend on the coordinate along the focus line in the scattering plane. The stationary phase method gives the possibility to find the correspondence between the different points on the topograph and on the surface of the crystal. This ray-approximation similar to geometrical optics will be called as a local approach.

4. The physical nature of the local approach.

Let us discuss the physical nature of the results, obtained by means of the stationary phase method. The relation (26) sets the connection between the points at the surface of the crystal (lens), at the source plane and at the observation planes. This relation with account of (14), (25), (27) can be rewritten in a more clear form

$$\xi(x) = L_1\,[\,\psi_0(x - x_d) + \psi_1(x - x_0, d)\,] + x\gamma_1\,, \tag{30}$$

where $x_0 = d\,c_1/\gamma_1$, $x_d = d\gamma/\gamma_0\gamma_1$, and

$$\psi_0(x) = \frac{\gamma_0^2}{\gamma_1 L_0}\left(x - \frac{\xi_s}{\gamma_0}\right) + \frac{\delta}{\gamma_1}(c_1 - c_0)\,,$$

$$\psi_1(x,z) = -\frac{1}{\gamma_1 R_c}\left[x(\gamma_0+\gamma_1) + (z - \frac{t}{2})\,(c_1 - c_0)\right] =$$

$$= -\frac{1}{\gamma_1 K}\,\frac{d\boldsymbol{h u}(x,z)}{dx}\,. \tag{31}$$

are the angular deviations of the local ray at the point x from the reference direction determined by the vector $\boldsymbol{k}_1$.

The relation (30) can be interpreted in the frame of geometrical optics approach of X-ray diffraction in disturbed crystals [12]. In this approach the crystal is considered as having a variable reciprocal lattice vector

$$\boldsymbol{h}(x,z) = \boldsymbol{h} - \frac{d\boldsymbol{h u}(x,z)}{dx}\,\boldsymbol{X} + \varepsilon \boldsymbol{Z}\,, \tag{32}$$

where $\boldsymbol{X}$, $\boldsymbol{Z}$ are the unit vectors along the X and Z axes, a parameter ε is unessential for our consideration.

Let us consider first the region of the crystal surface at the top of the relief where $d = 0$. Then at the point x the local wave vector of an incident ray is

$$\boldsymbol{k}'_0(x) = \boldsymbol{k}_0 + K \left[\frac{\gamma_0^2}{L_0} \left(x - \frac{\xi_s}{\gamma_0} \right) - \delta c_0 \right] \boldsymbol{X} + K\,\beta\,\boldsymbol{Z} \tag{33}$$

where β is determined from the condition $\boldsymbol{k}'^2_0 = (2\pi/\lambda)^2$. The x-projection of the local wave vector $\boldsymbol{k}'_0(x)$ can be obtained directly from (6).

The wave vector of the reflected ray is

$$\begin{aligned} &\boldsymbol{k}'_1(x) = \boldsymbol{k}'_0(x) + \boldsymbol{h}(x,0) + Kf\boldsymbol{Z} = \boldsymbol{k}_1 + \\ &+K \left[\left(\frac{\gamma_0^2}{L_0} \left(x - \frac{\xi_s}{\gamma_0} \right) - \delta c_0 \right) - \frac{1}{K} \frac{d\boldsymbol{hu}(x,0)}{dx} \right] \boldsymbol{X} + Kf\boldsymbol{Z}\,. \end{aligned} \tag{34}$$

Here f is determined from the condition $\boldsymbol{k}'^2_1 = (2\pi/\lambda)^2 \approx K^2(1-2\delta)$. As a result one has

$$f = \left(\frac{\gamma_0^2}{L_0} \left(x - \frac{\xi_s}{\gamma_0} \right) - \frac{1}{K} \frac{d\boldsymbol{hu}(x,0)}{dx} \right) \frac{c_1}{\gamma_1} + \delta\, \frac{1 - c_0 c_1}{\gamma_1} \tag{35}$$

To obtain the shift of the point at the topograph one must find the transversal component of $\boldsymbol{k}'_1$ which determines the angular deviation of the local ray. It equals obviously $\Delta k'_{1\perp} = \Delta k'_{1x} \sin\theta_1 + \Delta k'_{1z} \cos\theta_1$. After a simple calculation one has

$$\Delta k'_{1\perp} = K\,[\,\psi_0(x) + \psi_1(x,0)\,]\,. \tag{36}$$

Thus the first term in (30) is really due to the angular deviation of the reflected ray from the basic direction which is determined by the vector $\boldsymbol{k}_1$ and the second term is simply the projection of the point at the surface to the film plane with a use of the $\boldsymbol{k}_1$ direction. This situation is illustrated by the Fig.2. The angular deviation depends on the incident ray direction (the function ψ_0) and on the local reciprocal lattice vector value (the function ψ_1).

It is clear that at the bottom of the surface relief the inlet and outlet points of the reflected ray are divided by the distance x_d. For the outlet point x the local incident ray is determined by the point $x - x_d$. It is due to the fact that the real reflection occurs at the point $x - x_0$ and at the depth d (see Fig.3). That is why the arguments of the ψ_1 function correspond to the real reflection point.

The relations (30), (31) allow to consider the lens of finite longitudinal length and clearly show the role of the waveband of the incident radiation. Namely, in the case of the symmetrical reflection $\theta_1 = \theta_0$ the wavelength shift leads to the topodraph image at the same place. A shift of the wavelength leads to the different reflectivity and to the different additional phase due to the surface relief but the location of the image is conserved the same. On the contrary in an asymmetrical case the lens of short length will give the image (a focusing strip) with the length much larger than the usual projection if the incident radiation has the wide wavelength band.

5. Sagittal focusing by Bragg-Fresnel lens.

The Eq.(28) allows to analyse the focusing effect in y-direction by means of the special phase zone surface relief where d depends on y according to the law

$$d\,(y) = \begin{cases} 0 & \sqrt{\lambda L_f\,(2n)} < |\,y\,| < \sqrt{\lambda L_f\,(2n+1)} \\ d & \sqrt{\lambda L_f\,(2n+1)} < |\,y\,| < \sqrt{\lambda L_f\,(2n+2)} \\ d & \sqrt{2N_r \lambda L_f} < y \\ d & y < -\sqrt{2N_l \lambda L_f} \end{cases} \tag{37}$$

Here λ is a wavelength, L_f is the focus distance of the lens. This profile is usually obtained by etching the surface. Below in this section the parameter d will be considered as a constant.

So called zero order intensity is obtained when the total surface is placed at $z = d$ independently on y. In this case R and φ_{fre} functions do not depend on y and the remained exponent function can be integrated analytically.

$$C_0(\xi, \eta) = \frac{\gamma_1}{\gamma_0} \frac{F_{inv}(\xi)\, F_{sph}(\eta - \eta_s)}{\sqrt{L_x\, L_y}}\, R\,(q_s(\xi, d))\, \exp\{-i\varphi_{fre}(\xi, d)\,\}\,, \tag{38}$$

where $L_y = L_0 + L_1$ and $F_{sph} = \exp(iK\eta^2/2L_y)$ is a standard phase multiplier for a spherical wave on the distance L_y in the small angle approximation.

In the places without etching the R-function has argument $q_s(\xi, 0)$ and the additional phase $-\varphi_{fre}\,(\xi, d)$ is absent. For calculating the intensity with the surface relief (37) it is convenient to replace the variables of integration $y = \sqrt{\lambda L_f}\, t$, and to write the expression for the reflected field as follows

$$C(\xi,\eta) = C_0(\xi,\eta)\,[\,1 + A\,(\xi)\,B\,(\eta)\,] \tag{39}$$

where

$$\begin{aligned}
A\,(\xi) &= \left(\frac{L_f}{i\,L_r}\right)^{\frac{1}{2}} (\,\Delta\,(\xi) - 1\,)\,, \\
\Delta\,(\xi) &= \frac{R\,(q_s(\xi,0))}{R\,(q_s(\xi,d))}\,\exp\,(i\,\varphi_{fre}(\xi,d)\,)\,, \\
B(\eta) &= \sum_{n=0}^{N_l-1}\int_{\sqrt{2n}}^{\sqrt{2n+1}} dt\,\exp\{ia\,(t+b\eta')^2\} + \\
&\qquad + \sum_{n=0}^{N_r-1}\int_{\sqrt{2n}}^{\sqrt{2n+1}} dt\,\exp\{ia\,(t-b\eta')^2\}\,.
\end{aligned} \tag{40}$$

Here $a = \pi\,L_f/L_r$, $b = L_r\,(L_1\sqrt{\lambda L_f}\,)^{-1}$, $\eta' = \eta + \eta_s\,L_1/L_0$, $L_r = L_0 L_1/L_y$ and N_l is the number of teeth at the left side of the lens while N_r is the same number at the right side.

The function $B(\eta)$ can be expressed through the Fresnel integrals (see, for example, [20])

$$\begin{aligned}
F(z) &= C(z) + i\,S(z) = \int_0^z dt\,\exp\left(i\,\frac{\pi}{2}\,t^2\right), \qquad z > 0\,, \\
F(z) &= -F(-z), \qquad z < 0\,.
\end{aligned} \tag{41}$$

by the next way

$$\begin{aligned}
B(\eta) = \frac{1}{\alpha}\Bigg(&\sum_{n=0}^{N_l-1}\Big[F(\alpha\,(\sqrt{2n+1}+b\eta')\,) - F(\alpha\,(\sqrt{2n}+b\eta')\,)\Big] + \\
+ &\sum_{n=0}^{N_r-1}\Big[F(\alpha\,(\sqrt{2n+1}-b\eta')\,) - F(\alpha\,(\sqrt{2n}-b\eta')\,)\Big]\Bigg)\,.
\end{aligned} \tag{42}$$

where $\alpha = \sqrt{2\,a/\pi} = \sqrt{2\,L_f/L_r}$. For the purpose of computer simulation the Fresnel integrals can be calculated by means of the computer's procedures S20ACE, S20ADE of the NAG library of the FORTRAN subroutines.

As follows from (39), (40) the focusing in η-direction by the Bragg-Fresnel lens is determined by the two conditions. Firstly, the zero order intensity $|\,C_0\,|^2$ must be large enough and, secondly, the phase difference

φ_{fre} has to be close to $-n\pi$ $(n = 1, 3, ..)$ at the same ξ point. The value of $|\,C_0\,|^2$ is determined mainly by the Bragg reflectivity of the lens. So at ξ point the reflectivity corresponds to the angular argument $q_s(\xi, 0)$. The reflectivity depends effectively on the parameter σ_0 which can be written by means of variable ξ as follows

$$\sigma_0 = w(\xi - \xi_{m\lambda} - \xi_{ms} - \xi_s')\,, \qquad \xi_{ms} = \frac{X}{w}\,, \tag{43}$$

where the notations are defined by (29). Since the centre of the total reflection region in the Bragg case is shifted from the zero point determined by the Bragg condition in the air and is determined from the condition $\sigma_0 = 0$ (see Eq.(21)) the maximum intensity on the topograph corresponds to the point $\xi = \xi_{ms} + \xi_{m\lambda} + \xi_s'$.

On the other hand the effect of focusing depends on the value of the phase difference. The Eq.(29) shows that $\varphi_{fre}(\xi, d) = -\pi\, n$ ($n =$ 1, 3, ...) when $\xi = -\pi\,(n - \varepsilon(d)\,)/wd + \xi_{m\lambda} + \xi_s'$. Therefore the strong focusing with the maximum reflectivity corresponds to the condition $X = -\pi\,(n - \varepsilon(d))/d$.

This condition determines a proper height of the teeth for a good focusing

$$d = \frac{\lambda\,\gamma_0\,\gamma_1}{|\chi_0|\,(\gamma_0 + \gamma_1)}\,(n - \varepsilon(d))\,. \tag{44}$$

The Eq.(44) means that the condition of good focusing does not depend on the distances L_0, L_1 and R_c as well as on the wavelength shift δ and ξ_s. The latter is due to the fact that the function $A(\xi)$ depends effectively on $\xi - \xi_{m\lambda} - \xi_s'$. Therefore the condition of good focusing is the same for different δ and ξ_s but the focusing effect takes place at different ξ-points.

The additional phase difference may arise from the shift of the argument of the reflection amplitude $\Delta q_s = q_s(\xi, 0) - q_s(\xi, d)$. In terms of ξ-dependence Δq_s corresponds to ξ_d. In the conditions far off the focusing, where L_x does not equal zero, the parameters ε and ξ_d are small and do not influence the effect.

Although formally the focusing effect takes place for all values of ξ (focus spot has the form of a strip) the region of maximum focal intensity for infinite lens is limited by both the width of the crystal rocking curve and the region where the phase $\varphi_{fre}(\xi, d)$ is close to $-\pi$. The focusing effect can occur also at the tails of rocking curve where $\varphi_{fre}(\xi, d) \approx$ π, -3π, 3π, -5π, $\cdots$ with a small reflectivity. For the real lens of the finite length the length of the focusing strip is limited by the length of the lens.

Now let us consider the function $B(\eta)$ describing the focusing effect. The important condition is $L_f = L_r\, n$, $n = 1,\, 3,\, 5\ldots$ for a good focusing of n-th order. It means that the first order focus distance L_1 must be slightly larger than L_f when L_0 is large, namely,

$$L_1 = \frac{L_f}{n}\,\frac{L_0}{(L_0 - L_f/n)}\,. \tag{45}$$

A shift of the point source on the distance η_s relative the lens centre leads to a shift of the image in the topograph on the distance $\eta = -\eta_s\, L_1/L_0$ (in the opposite direction). So for $L_1 \ll L_0$ one obtains the focus of much smaller dimension as compared with the source dimension.

In the experiments the lens of finite length D_x and the radiation of relatively wide waveband D_δ are usually used. Then the effective image size at the topograph in a meridional direction according to (30), (31) equals

$$D_\xi = \frac{L_x \gamma_0^2}{L_0 \gamma_1}\, D_x + \frac{(c_1 - c_0)}{\gamma_1}\, L_1 D_\delta\,. \tag{46}$$

On the other hand as follows from (29), (43) the intensity in each ξ-point contains the contributions which corresponds to other ξ-points shifted due to the wavelength change by $\xi_{m\lambda}$. The total interval of averaging is $\Delta\xi = (\partial\xi_{m\lambda}/\partial\delta)\, D_\delta$. The parameter $\xi_{m\lambda}$ (29) can be written in the form

$$\xi_{m\lambda} = \frac{(c_1 - c_0)}{\gamma_1}\, L_1\delta_1 - L_x\left(A\delta + B\,\frac{t}{2R_c}\right)\,, \tag{47}$$

where

$$A = \frac{\gamma_0 \mathrm{tg}\theta_B}{\gamma_1 M_0}\,, \qquad B = \frac{\gamma_0}{\gamma M_0}\left[\frac{c_1(c_1 - c_0)}{\gamma_1} - a_0 - a_1\right]\,. \tag{48}$$

As follows from these formulae in the symmetrical case $\theta_0 = \theta_1$ the image size does not depend on waveband but the interval of averaging equals $\Delta\xi \approx A L_x D_\delta$ and does not turn to zero if the meridional focusing condition ($L_x = 0$) is not met. So the strip of homogeneous darkness should be observed in the topograph with the intensity which is the integral over the ξ intensity. The source size plays just the same role. Just the topographs with such structure of focus line were observed in the experimental works [3-10].

6. Meridional focusing by elastically bent crystal.

As follows from (30), (31) the point $\xi(x)$ at the topograph is independent on x if the following condition is fulfilled

$$\frac{\gamma_0^2}{L_0} + \frac{\gamma_1^2}{L_1} = \frac{\gamma_0 + \gamma_1}{R_c} \,. \qquad (49)$$

In this case all the incident rays are gathered with the very high intensity at one and the same point

$$\xi_f = \frac{L_1}{\gamma_1}\,(c_1 - c_0)\,\delta_t + d\,\frac{\gamma}{\gamma_0}\left(1 - \frac{L_1}{\gamma_1 R_c}\right) - \xi_s\,\frac{\gamma_0 L_1}{\gamma_1 L_0} \qquad (50)$$

As follows from (50) the regions at the top and at the bottom of the tooth gather the radiation at different points.

It is clear that under the condition (49) the phase Ψ in (24) does not contain the terms of x^2 and the stationary phase method is invalid. Formally the expression (28) is infinite because the parameter $L_x = 0$. If $M_0 \neq 0$ then the expression (24) is yet finite if it will be calculated explicitly. However, it gives the correct value only at the point $\xi = \xi_f$ because it corresponds to the ray approximation. To obtain the intensity at all the values of ξ under the condition (49) it is better to perform the calculation without the ray approximation at all. For this purpose one can substitute (22) in (7) and first calculate the integral over x. It can be performed accurately with a use of (17) in a suggestion of long enough lens. To eliminate the wavelength dependence of the reflectivity one can made in addition the shift of q variable by $q_\lambda = v\gamma_0\gamma_1/\gamma$ with v determined by (20). The result has the form

$$C(\xi,\eta) = \frac{F'_{inv}(\xi)}{\gamma_0\,(L_0 L_1 M_0 M_1)^{\frac{1}{2}}} \int dy\,\exp\{i\varphi_{tra}(y)\} \int \frac{dq}{2\pi}\,R(q - q_\lambda)\,\times$$
$$\times\,\exp\left(i\,\frac{\xi - \xi_{m\lambda} - \xi'_s - \xi_d}{\gamma_1 M_1}\,q - i\,\frac{L_x}{2K\gamma_1^2 M_0 M_1}\,q^2\right)\,, \qquad (51)$$

where

$$F'_{inv}(\xi) = F_0 F_1 F'_0 F'_1 \exp(-i\,\tfrac{1}{2}\,[\,\alpha_0(q_0^2 + q_\lambda^2) +$$
$$+\alpha_1(q_0^2 + q_\lambda^2)\,] - iq_\lambda(\xi - \xi_\lambda - \xi'_s)/\gamma_1 M_1) \qquad (52)$$

is a new invisible multiplier while other notations are determined by (14), (29).

This expression clearly shows that the intensity depends only on $(\xi - \xi_{m\lambda} - \xi_s')$ because the invisible exponent factor vanishes and $R(q - q_\lambda)$ does not depend on the wavelength and the source position. It means that the integration of the intensity over the wavelength band is equivalent to averaging the ξ-dependence. The surface relief, in general, leads to a change of both the phase and the amplitude of the field because the phase factor is under the integration sign.

The condition (49) is equivalent to $L_x = 0$. When this condition is not met the integral can be calculated by means of the stationary phase method with the result described by (28), (29). It is clearly seen from (51) that the cases where $M_0 = 0$ or $M_1 = 0$ have to be considered separately due to the formal divergences in the expressions. The case when the distances L_0, L_1 lie at the Rowland circle with the diameter R_c corresponds to $L_0 = \gamma_0 R_c$, $L_1 = \gamma_1 R_c$ that means in our notations $M_0 = M_1 = 0$ simultaneously. It is easy to see that the expression (51) becomes undetermined and for obtaining the accurate result we must use the following term of the expansions in (6), (8). Below these situations will not be considered. We shall assume that $M_0 \neq 0$, $M_1 \neq 0$ and only $M_0 = -M_1(\gamma_1^2 L_0)/(\gamma_0^2 L_1)$. In this case the focusing effect takes place and the intensity distribution can be calculated by means of (51). The integral over q becomes simply the Fourier image of the crystal reflectivity.

Let us consider now the sagittal focusing by Bragg-Fresnel lens under the condition of meridional focusing. For the $d(y)$ dependence described by (37) one can obtain the expression (39) once again but with the new values $C_0(\xi, \eta)$ and $\Delta(\xi)$, namely,

$$C_0(\xi,\eta) = \left(\frac{i\lambda}{L_y M_0 M_1}\right)^{\frac{1}{2}} \frac{F'_{inv}(\xi) F_{shp}(\eta - \eta_s)}{2\pi\gamma_0} F_R(\xi - \xi_{m\lambda} - \xi_s' - \xi_d)\,,$$

$$\Delta(\xi) = \frac{F_R(\xi - \xi_{m\lambda} - \xi_s')}{F_R(\xi - \xi_{m\lambda} - \xi_s' - \xi_d)}\,, \tag{53}$$

where

$$F_R(\xi) = \int dq\, R(q - q_\lambda) \exp\left(i \frac{\xi q}{\gamma_1 M_1} - i \frac{L_x}{2K\gamma_1^2 M_0 M_1} q^2\right)\,. \tag{54}$$

When $L_x = 0$ the function $F_R(\xi)$ is known to have the analytical expression [21]. Substituting (21) in (54) and taking into account (20) one obtains

$$F_R(\xi) = \pi i s \frac{\gamma_0\gamma_1}{\gamma} \exp\left(i \frac{\gamma_0 X}{\gamma M_1} \xi\right) F_B\left(\frac{s\sqrt{f}\gamma_0}{\gamma M_1} \xi\right) \theta\left(\frac{\xi}{M_1}\right)\,, \tag{55}$$

where

$$F_B(x) = \mathrm{J}_0(x) + \mathrm{J}_2(x) = \frac{2\mathrm{J}_1(x)}{x}\,, \tag{56}$$

and $\mathrm{J}_n(x)$ is the Bessel function of order n. The function $\theta(x)$ equals to unity if $x > 0$ and zero otherwise. This expression reads that the intensity distribution inside the focal spot is asymmetrical with abrupt low ξ side. The width of focus is about micrometer. So the surface relief can really give the focuses in different places by it's top and bottom fragments for rather large height d. In this case the Fresnel focusing becomes the amplitude focusing instead of the phase one.

7. Numerical example

The formulae obtained in the previous sections allow to calculate the detailed distibution of the intensity on the topograph under any conditions which include the condition of focusing as a particular case. For the long enough lens the formulae (53), (54) are the more general. These describe the intensity distribution for an arbitrary angular dependence of the crystal reflectivity including the deformations due to bending as well as due to any external deformations, for example, after the ion implantation of the crystal surface. In this section the results of numerical calculation based on the Eqs. (39), (40), (53), (54) are presented for the reflectivity described by (21). More complicated cases will be considered in the following publications. As an example the case of Si, 111, $\gamma_0 = \gamma_1 = 0.1977$, $\lambda = 1.24$ Å$(E = 10keV)$, $L_0 = 50m$, $L_f = 0.5m$, $N_l = N_r = 30$ has been calculated. For these values of free parameters the remained parameters can be determined from the conditions of good focusing. So we find from (44) $d = 1.255$ Å, and from (45) $L_1 = 0.505m$.

The results of calculation for these conditions and the flat crystal ($R_c = \infty$) are shown in the Fig. 4. The monochromatic spherical wave is assumed as an incident wave. The intensity is related to the intensity of the spherical wave in a free space at the distance $L_0 + L_1$ from the source. One can see that the width of the focus line is about 0.5 μm and the focus has the form of very long but finite strip with the inhomogeneous intensity along the strip. The total longitudinal size of the focus is defined by the width of the reflectivity curve (the Darwin table) but the characteristic sinusoidal form of the intensity distribution is determined by the linear dependence of the phase difference φ_{fre} on ξ with the maximum intensity when $\varphi_{fre} = -\pi$. The intensity at the focus increases by a factor 90 that coincides approximately with the estimation $16(N_l + N_r)/\pi^2$ given in [9]. The calculation in the ray approximation (Eqs. (25), (38), (40)) gives the quitely identical result for this case. It is of interest to notice that large values of the teeth height d lead to the very fast dependence of the phase difference φ_{fre} on ξ so that φ_{fre} can take the values -3π, $-\pi$, π within the Darwin table. In this case the intensity distribution along the focus line will have few maximums separated by minimums.

Fig. 5 shows the results of calculation under the conditions of double focusing when, according to (49) $R_c = 5.06m$. In this case the maximum of the relative intensity (the gain) equals 1500. The focus has the longitudinal size of about 3 μm independently on L_0 and a rather complicated form which involves two peaks. The peaks have a sharp low ξ side but not the abrupt one. It is due to the approximate calculation of the integral in the limits of three Darwin table widths and without small and long tails of the reflectivity curve. The first peak corresponds to a pure amplitude focusing by the top of teeth of the surface relief. The rays reflected by the bottom of the relief cannot pass to this point of the topograph. The second peak is formed by the interference between rays reflected by the top and the bottom of the structure but with different amplitudes due to the different focusing conditions. In this case the result depends on the phase difference as well.

Acknowledgments

The author would like to thank Dr. A. Snigirev, Dr. Ya. Hartman and Dr. I. Snigiveva for the idea of this work and helpful discussions and Prof. G. V. Smirnov for the critical reading the manuscript and useful remarks.

Appendix

We shall find the solution of the Eq.(19) in the form $R(z) = B(z)/A(z)$. Then this equation can be divided on two equations

$$\frac{dA}{dz} = \frac{i}{2}\left[-\sigma A + sf B\right], \qquad \frac{dB}{dz} = \frac{i}{2}\left[\sigma B - s A\right], \tag{A1}$$

where $\sigma = \sigma_0 - \sigma_1 z$. The next step is a transition from the two equations with the first order derivatives to one with the second order derivative for each function $C = A, B$ separately

$$\frac{d^2C}{dz^2} = \frac{1}{4}\left(\mp 2i\sigma_1 - s^2 f + \sigma^2\right) C\,. \tag{A2}$$

Here and below the upper sign is for A and the lower sign is for B. By the substitution $z \to Z$ this equation can be transformed to

$$\frac{d^2C}{dZ^2} - \left(a + \frac{Z^2}{4}\right) C = 0 \tag{A3}$$

where

$$Z = \frac{\sigma_0 - \sigma_1 z}{\sqrt{i\sigma_1}}\,, \qquad a = \nu \mp \frac{1}{2}\,, \qquad \nu = \frac{is^2 f}{4\sigma_1}\,. \tag{A4}$$

The Eq.(A3) is a standard form of the equation for the special function of parabolic cylinder [20]. As a result the solution of (19) can be written by means of the Weber function $D_n(x)$ in the form $R(z) = D_{-\nu-1}(Z)/D_{-\nu}(Z)$.

Reference

[1] V.V.Aristov, A.A.Snigirev, Yu.A.Basov, A.Yu.Nikulin, AIP Conf. Proc., 147, 253, 1986.

[2] V.V.Aristov, Yu.A.Basov, S.V.Redkin, A.A.Snigirev, V.A.Yunkin, Nucl. Instr. Meth. A261, 72, 1987.

[3] V.V.Aristov, Yu.A.Basov, G.N.Kulipanov, V.F.Pindyurin, A.A.Snigirev, A.S.Sokolov, Opt. Commun. 66, 183, 1988.

[4] V.V.Aristov, Yu.A.Basov, G.N.Kulipanov, V.F.Pindyurin, A.A.Snigirev, A.S.Sokolov, Nucl. Instr. Meth. A274, 390, 1989.

[5] V.V.Aristov, Yu.A.Basov, A.A.Snigirev, Rev. Sci. Instr. 60, 1517, 1989.

[6] Yu.A.Basov, T.L.Pravdivtseva, A.A.Snigirev, M.Belakhovsky, P.Dhez, A.Freund, Nucl. Instr. Meth. A308, 363, 1991.

[7] U.Bonse, C.Riekel, A.A.Snigirev, Rev. Sci. Instr. 63, 622, 1992

[8] V.V.Aristov, Yu.A.Basov, A.A.Snigirev, V.A.Yunkin, Rev. Sci. Instr. 63, 586, 1992

[9] V.V.Aristov, Yu.A.Basov, T.E.Gureev, A.A.Snigirev, T.Ishikawa, K.Izumi, S.Kikuta, Jpn. J. Appl. Phys. 31, 2616, 1992.

[10] A.Snigirev, Rev. Sci. Instr. 66, 1, 1995

[11] Ya.Hartman, A.Freund, I.Snigireva, A.Snigirev, Nucl. Instr. Meth. 1995, to be published

[12] Z.G.Pinsker, Dynamical Scattering of X-Rays in Crystals (Springer, Heidelberg) 1984.

[13] K.T.Gabrielyan, F.N.Chukhovskii, D.I.Piskunov, Zh. Exper. Teor. Fiz. 96, 834, 1989.

[14] F.N.Chukhovskii, W.Z.Chang, E.Förster, J. Appl. Cryst. 27, 971, 1994

[15] A.M.Afanas'ev, V.G.Kohn Fiz. tverdogo tela 1977, 19, 1775

[16] J.M.Cowley, Diffraction physics, North-Holland, Amsterdam, American Elsevier, N.Y., 1975.

[17] I.Uschmann, F.Förster, K.Gäbel, G.Hölzer, M.Ensslen, J. Appl. Cryst. 26, 405, 1993.

[18] F.N.Chukhovskii, K.T.Gabrielyan, P.V.Petrashen', Dokl. Akad. Nauk SSSR, 238, 31, 1978.

[19] F.N.Chukhovskii, K.T.Gabrielyan, P.V.Petrashen', Acta Cryst., A34, 610, 1978.

[20] Handbook of mathematical functions, 1964, Eds. M.Abramowitz and I.A.Stegun. Applied Mathematic Serie •55

[21] A.M.Afanas'ev, V.G.Kohn Acta Cryst. A27 421, 1971.

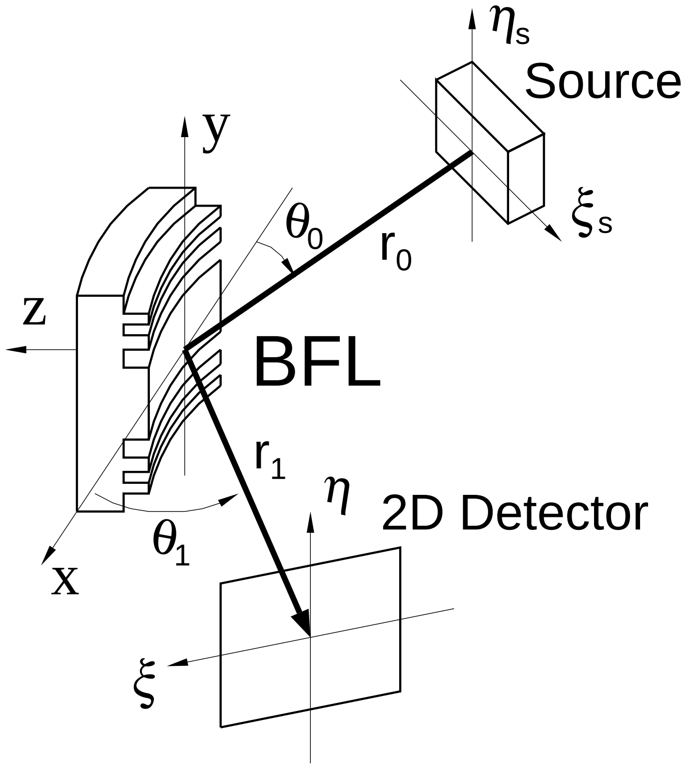

Figure 1: Experimental arrangement and geometrical parameters.

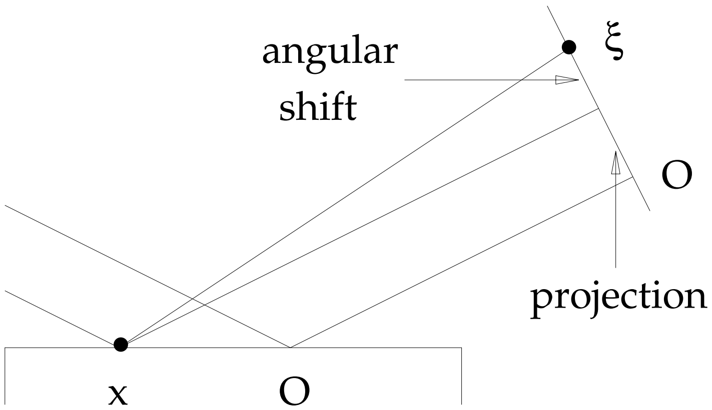

Figure 2: Correspondence between points at the crystal surface and at the topograph.

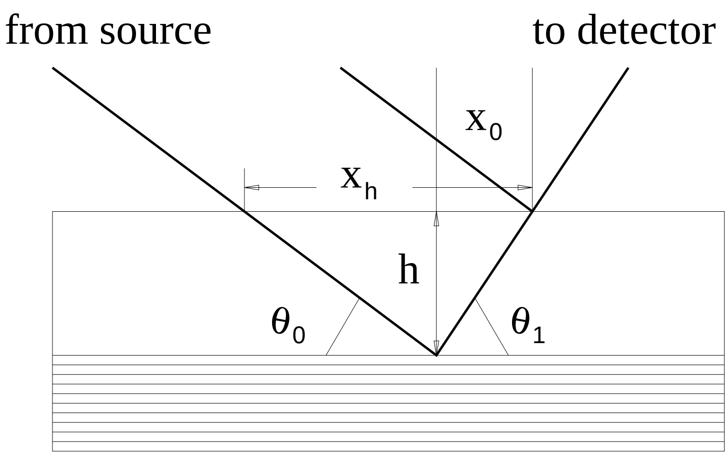

Figure 3: Path of the ray between teeth of surface relief.

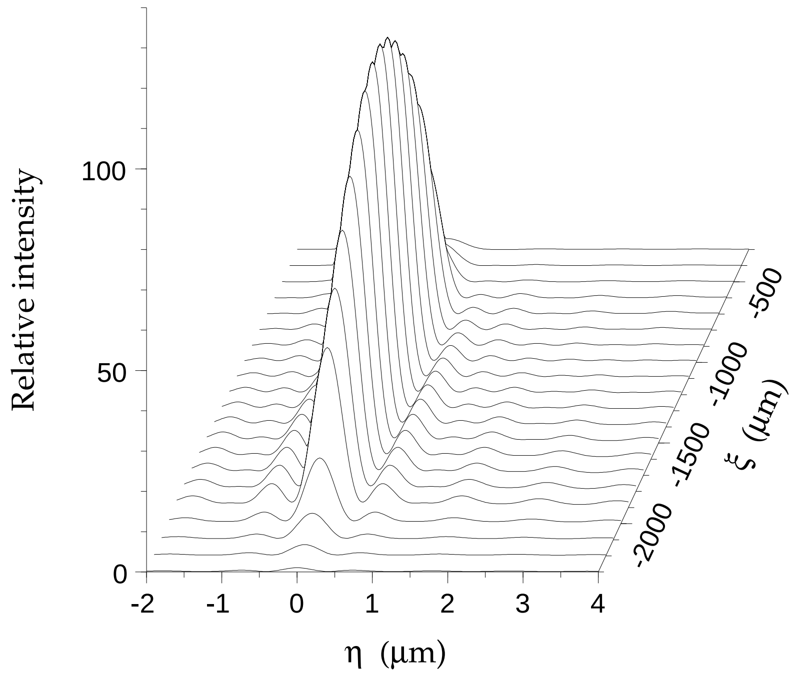

Figure 4: Intensity distribution for a flat lens. Si, 111, $E = 10$ keV, $L_f = 0.5$ m.

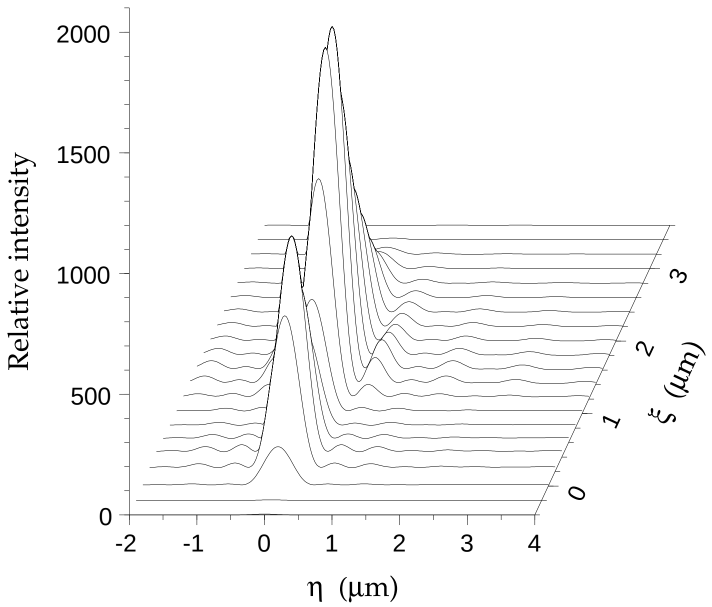

Figure 5: Double focus for a bent lens. Si, 111, $E = 10$ keV, $L_f = 0.5$ m, $R_c = 5.06$ m.

Технический редактор О. П. Громова

Подписано в печать 28.04.95. Формат 60x90/16
Печать офсетная. Усл. печ. л. 1,5. Уч.-изд. л. 1,5
Тираж 68. Заказ 49. Индекс 3624.

Отпечатано в РНЦ "Курчатовский Институт"
123182, Москва, пл. Академика Курчатова

Preprint IAE-5878/9, M., 1995.